

# Two-center Interferences in Photoionization of Dissociating $\text{H}_2^+$ Molecule

A. Picón<sup>1</sup>, A. Bahabad<sup>1,2</sup>, H.C. Kapteyn<sup>1</sup>, M.M. Murnane<sup>1</sup>, and A. Becker<sup>1</sup>

<sup>1</sup> *JILA and Department of Physics, University of Colorado at Boulder, Boulder, Colorado 80309-0440, USA*

<sup>2</sup> *Department of Physical Electronics, School of Electrical Engineering, Tel-Aviv University, Tel-Aviv, 69978, Israel*

(Dated: March 6, 2022)

We analyze two-center interference effects in the yields of ionization of a dissociating hydrogen molecular ion by an ultrashort VUV laser pulse. To this end, we performed numerical simulations of the time-dependent Schrödinger equation for a  $\text{H}_2^+$  model ion interacting with two time-delayed laser pulses. The scenario considered corresponds to a pump-probe scheme, in which the first (pump) pulse excites the molecular ion to the first excited dissociative state and the second (probe) pulse ionizes the electron as the ion dissociates. The results of our numerical simulations for the ionization yield as a function of the time delay between the two pulses exhibit characteristic oscillations due to interferences between the partial electron waves emerging from the two protons in the dissociating hydrogen molecular ion. We show that the photon energy of the pump pulse should be in resonance with the  $\sigma_g - \sigma_u$  transition and the pump pulse duration should not exceed 5 fs in order to generate a well confined nuclear wavepacket. The spreading of the nuclear wavepacket during the dissociation is found to cause a decrease of the amplitudes of the oscillations as the time delay increases. We develop an analytical model to fit the oscillations and show how dynamic information about the nuclear wavepacket, namely velocity, mean internuclear distance and spreading, can be retrieved from the oscillations. The predictions of the analytical model are tested well against the results of our numerical simulations.

PACS numbers: 33.80.Rv, 42.25.Hz, 42.50.Hz

## I. INTRODUCTION

Double-slit like interferences similar to those observed by Young in his experiment with light [1] occur also in the (photo-)ionization of diatomic molecules. Conceptually, the partial electron waves ejected from the two atomic centers of the molecule take the role of the coherent light waves emerging from the two holes in Young's experiment. The phenomenon was first discussed by Cohen and Fano [2] to explain the observation of oscillations in the total photoionization cross section of the  $\text{H}_2$  molecule as a function of the photon energy [3]. According to their analysis, the interference pattern depends periodically on the ratio of the internuclear distance to the wavelength of the photoelectron and is superimposed on the quickly decreasing photoabsorption cross section. In recent years, Young-type interferences have been observed experimentally and studied theoretically for the photoemission of (core) electrons from  $\text{H}_2^+$  and  $\text{H}_2$  [4–10] and heavier molecules [11–14]. Furthermore, interference effects in the ionization of molecules by heavy ion [15, 16] and electron impact [17, 18] have been investigated. Recently, the idea of Cohen and Fano was extended to the double photoionization of  $\text{H}_2$  [19–23], the photoionization of more complex molecules [24], and laser induced multiphoton ionization of molecules [25, 26].

In photoionization of a diatomic molecule the double-slit interferences primarily depend on the momentum of the photoelectron,  $k$ , the internuclear distance between the two atoms,  $R$ , and the angle between the emission direction of the electron and the molecular axis. In past work, photoionization of molecules from the ground electronic state and corresponding interference patterns in the angular distributions of the photoelectron in the

molecular body fixed frame was studied. Even the small variations of the internuclear distance in the vibrational states of a bound molecule could be observed in the patterns [14, 23].

However, the dependence of the interference patterns on the internuclear distance becomes more apparent in the photoionization from dissociating molecules. In a recent set of experiments negative iodine molecules  $\text{I}_2^-$  were excited by a pump laser pulse to a dissociative state, in which the molecule fragments into a negative ion  $\text{I}^-$  and a neutral atom I [27–29]. During the dissociation the molecule was ionized by a second pump laser pulse and the photoelectron spectra were measured. The anisotropy parameter obtained from the photoelectron angular distributions was found to oscillate as a function of the pump-probe time delay, in other words as a function of the increasing internuclear distance in the dissociating molecule. As in the previous examples, the oscillation arises due to the interference between the partial electron waves emerging from the two fragments.

Very recently, the probe step in such kind of pump-probe experiments, namely the photoionization of the dissociating molecule, has been studied theoretically using first-order perturbation theory for the prototype example of a  $\text{H}_2^+$  molecular ion, where the positions of the nuclei were fixed at different internuclear separations [30]. Assuming a nuclear wave packet of Gaussian shape with a certain but fixed width  $\Delta R$  centered at an internuclear distance  $R_0$ , the angular and momentum distribution of the photoelectron emitted from the first excited electronic state ( $\sigma_u$ -orbital) of  $\text{H}_2^+$  was calculated. The two-slit interferences were explored for different orientations of the molecular axis with respect to the polarization direction of the probe laser.

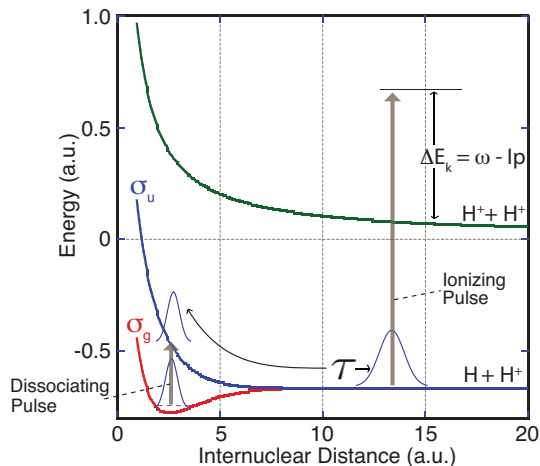


FIG. 1: (Color online) Scheme of the pump-probe scenario, in which a first (pump) pulse initiates the dissociation by excitation of a wavepacket to the  $\sigma_u$ -state of  $\text{H}_2^+$ . With a time delay  $\tau$  a second (probe) pulse ionizes the dissociating molecular ion. The green curve denotes the energy of two protons as a function of internuclear distance.

In the present work we complement this recent theoretical study by results of numerical simulations in which we investigate the complete pump-probe scenario according to the following scheme (see Fig. 1 for illustration). We consider a  $\text{H}_2^+$  molecular ion initially prepared in its electronic ( $\sigma_g$ ) and vibrational ( $\nu = 0$ ) ground state. The interaction with an ultrashort pump pulse resonantly excites part of the wave packet into the repulsive  $\sigma_u$ -state, thus initiating the dissociation of the molecule. The ungerade state corresponds to an antisymmetric electronic wave function consisting of a coherent superposition of atomic orbitals localized at the two dissociating protons, which establishes a double-slit scenario. During the dissociation the protons first accelerate in the steep part of the molecular ion potential and then propagate with almost constant velocity. Furthermore, the width of the nuclear wave packet increases as a function of internuclear distance due to dispersion. This requires to generate a well-confined nuclear wave packet in the excitation (pump) step in order to resolve the interferences in the ionization yields, as we will show below. In our simulations, we then modeled the interaction of the dissociating molecular ion with a second ultrashort probe laser pulse to determine the ionization probability as a function of the time delay between the dissociating and ionizing pulses. As we will show below, our results exhibit the expected Young-type interferences. We finally develop an analytical model in order to use such observations as an imaging tool for the velocity, internuclear distance and the spread of the nuclear wave packet.

The paper is organized as follows. In section II we introduce the  $\text{H}_2^+$  model ion used to perform the numerical simulations. Then, in section III we study the dissociation of the  $\text{H}_2^+$  model ion by the pump pulse and dis-

cuss the analogy of the probability density distribution of the dissociating system to a two-slit scenario for different parameters of the pump pulse. Next, results for the ionization yields will be presented in section IV, where the double-slit interference patterns will be identified and analyzed in view of imaging the characteristic features of the nuclear wave packet. Finally, we conclude with a short summary.

## II. $\text{H}_2^+$ MODEL FOR NUMERICAL SIMULATIONS

For our analysis of the ionization of the dissociating hydrogen molecular ion following the pump-probe scheme, illustrated in Fig. 1, we make use of a model for  $\text{H}_2^+$  in which the electronic and nuclear motion are restricted to one dimension. The model accounts for the interaction of the electron with the external fields as well as for non-Born-Oppenheimer effects. In the model, the polarization direction of the two linearly polarized pump and probe laser pulses coincide with the internuclear axis of the molecular ion as well as with the restricted electronic motion. The field-free Hamiltonian of this model system is given by (we use Hartree atomic units,  $e = m = \hbar = 1$ ) [31, 32]:

$$\hat{H}_0 = \frac{\hat{P}^2}{2\mu_R} + \frac{\hat{p}^2}{2\mu_z} + \frac{1}{\sqrt{R^2 + \alpha_p}} - \frac{1}{\sqrt{(z - R/2)^2 + \alpha_e}} - \frac{1}{\sqrt{(z + R/2)^2 + \alpha_e}} \quad (1)$$

where  $\hat{P} = -i\partial/\partial R$  and  $R$ , and  $\hat{p} = -i\partial/\partial z$  and  $z$  are the linear momentum operators and the positions of the relative nuclear (protons) and electronic coordinate, respectively.  $\mu_R = M/2$  and  $\mu_z = 2M/(M + 1)$  are the reduced masses where  $M = 1836$  a.u. is the mass of the proton. We have chosen soft-core parameters  $\alpha_e = 1$  and  $\alpha_p = 0.03$  [32]. The interaction of the electrons is taken into account in dipole approximation and velocity gauge by:

$$\hat{V}_I(t) = -(A_d(t) + A_i(t - \tau))\hat{p} \quad (2)$$

with

$$A_l(t) = \left(1 + \frac{1}{1 + 2M}\right) A_{0,l} \sin(\omega_l t) \sin^2(\pi t/N_l T_l) \quad (3)$$

where  $A_{0,l}$  is amplitude of the vector potential,  $\omega_l$  is the frequency of the carrier wave,  $N_l$  and  $T_l$  are the number of cycles and the period of the carrier wave of either the dissociating ( $l = d$ ) or the ionizing ( $l = i$ ) pulse, respectively, and  $\tau$  is the time delay between the two pulses.

The corresponding time-dependent Schrödinger equation

$$i \frac{\partial \psi(z, R, t)}{\partial t} = [\hat{H}_0 + \hat{V}_I(t)] \psi(z, R, t), \quad (4)$$

was solved using the Crank-Nicolson method [33]. The sizes of the simulation box were 1 to 37 a.u. and -409.6 a.u. to 409.6 a.u. in  $R$  and  $z$  direction, respectively, with a grid spacing of  $\Delta R=0.03$  a.u. and  $\Delta z=0.1$  a.u.. The time step in the simulations was  $\Delta t=0.02$  a.u.. The electronic-vibrational ground state of the model hydrogen molecular ion was obtained using imaginary time propagation, the ground state energy was -0.77 a.u., the equilibrium distance 2.6 a.u. and the ionization potential for  $R \rightarrow \infty$  about 0.71 a.u..

We have chosen to restrict the electronic motion to one dimension along the polarization axis and the internuclear axis in our model, since we analyzed the ionization of the dissociating hydrogen molecular ion up to rather large internuclear distances (37 a.u.) and used a largely extended grid in  $z$ -direction ( $> 800$  a.u.) in order to keep the wavefunction on the grid for further analysis. In recent studies, higher-dimensional calculations have been performed, in which the full three-dimensional electronic motion [10] or the two-dimensional electronic motion in cylindrical coordinates have been taken into account [34–37]. These higher-dimensional calculations are usually either performed on smaller grids or make use of high performance supercomputers. Here, we are interested in the analysis of the double-slit interference effects in the ionization signal from the dissociating molecular ion as a function of the internuclear distance  $R$ . These effects are expected to be present independent of the emission direction of the electron, which justifies a restriction of the electronic motion to one dimension.

### III. DISSOCIATION DYNAMICS

First, we analyze the dissociation dynamics of the hydrogen molecular ion after the interaction with the pump laser pulse. To this end, we performed numerical simulations of the model hydrogen molecular ion interacting with just one ultrashort laser pulse. We filtered out the electronic-vibrational ground state after the interaction and monitored the wavepacket in the excited state as a function of time. In Fig. 2 we compare two snapshots of the temporal evolution of the excited state probability density as a function of  $z$  and  $R$  (panels (b) and (c)) with the corresponding distribution in the ground state (panel (a)). The calculations were performed for a dissociating pump pulse with  $\omega_d = 0.38$  a.u. (period  $T_d = 16.22$  a.u.), corresponding to a central wavelength of 117 nm, which is resonant with the  $\sigma_g - \sigma_u$  transition in our model. The full pulse contained three cycles ( $N_l = 3$ ), i.e. a full pulse length of 48.66 a.u., about 1.2 fs. The amplitude of the vector potential was  $A_{0,d} = 0.04$  a.u., corresponding to a peak intensity of  $8.4 \times 10^{12}$  W/cm<sup>2</sup>. At the end of the pulse, the total excitation probability, i.e. the probability after projecting out the  $\sigma_g$  ground state, was 2.26%.

Fig. 2 shows, as expected, that the excited state probability density propagates to larger internuclear distances after the interaction with the pump pulse, which indi-

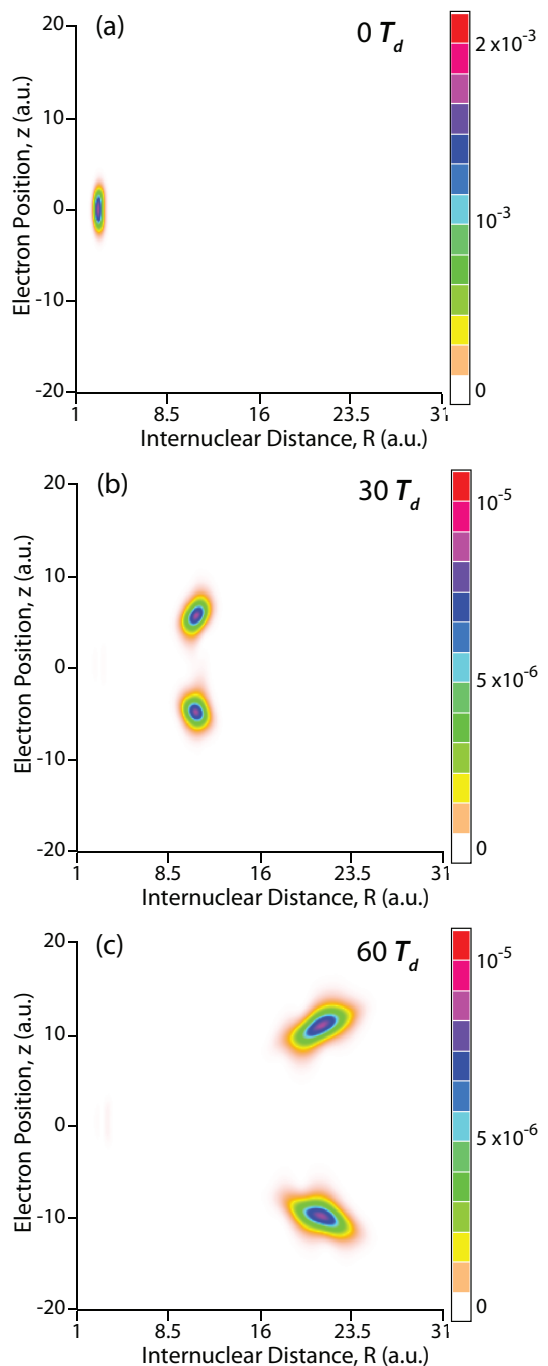


FIG. 2: (Color online) Comparison of the electron probability density in the ground state of the  $H_2^+$  model (panel (a)) with the temporal evolution of the density in the first excited state of hydrogen molecular ion following an excitation of the molecular ion by an ultrashort laser pulse with a central wavelength of 117 nm and a full pulse length of 48.66 a.u. (about 1.2 fs). Shown are snapshots of the excited state wavepacket density at (b)  $30T_d$  (11.782 fs) and (c)  $60T_d$  (23.564 fs).

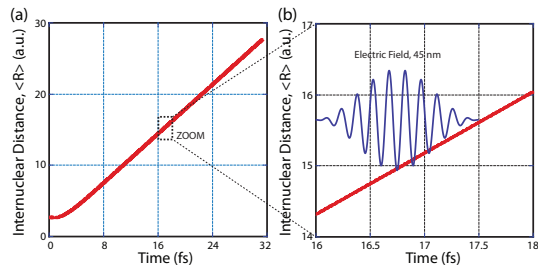


FIG. 3: (Color online) (a) Expectation value of the internuclear distance as a function of time. (b) Enlarged view of (a) for a time interval of 2 fs (16 fs to 18 fs). For the sake of comparison, we have also plotted the electric field of a 10-cycle pulse at a wavelength of 45 nm, which was used as a probe pulse below.

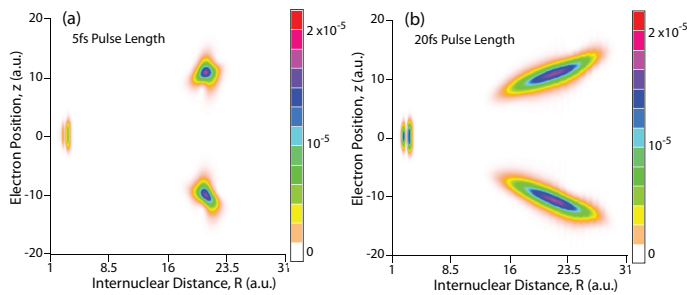


FIG. 4: (Color online) Electron probability density (after removal of the electronic-vibrational ground state) following the interaction with pump laser pulses at 117 nm having a full pulse length of (a) 5 fs at  $t = 61T_d$  (23.912 fs) and (b) 20 fs at  $t = 80T_d$  (31.360 fs).

icates a dissociation of the molecular ion. One sees that, at a given internuclear distance, the density is almost equally (de-)located at both protons and, hence, it forms the anticipated set-up, similar to a double slit. We note that the initially very well confined nuclear wave packet with a narrow distribution in  $R$  does spread significantly due to dispersion as the time proceeds.

Next, we present in Fig. 3 the result from the numerical simulations for the expectation value of the internuclear distance  $\langle R \rangle$  as a function of time after the interaction with the pump pulse. Please note that the expectation value was calculated after the remaining population in the ground state was removed. It is clearly seen that the wave packet gets accelerated over the first few femtoseconds due to the steep gradient of the repulsive potential energy curve for the  $\sigma_u$ -state at short internuclear distances. However, we observe that about 4-5 fs after the end of the interaction with the pump pulse the velocity of the wave packet is almost constant and  $\langle R \rangle$  increases linearly with time. From the expanded view in Fig. 3(b) we notice that the expectation value  $\langle R \rangle$  changes by 0.86 a.u. ( $\pm 0.02$  a.u.) within 1 fs in the linear regime, i.e. the nuclear wave packet propagates with a velocity of 0.0104 a.u. ( $\pm 0.0003$  a.u.).

We also studied the dissociation dynamics for pump

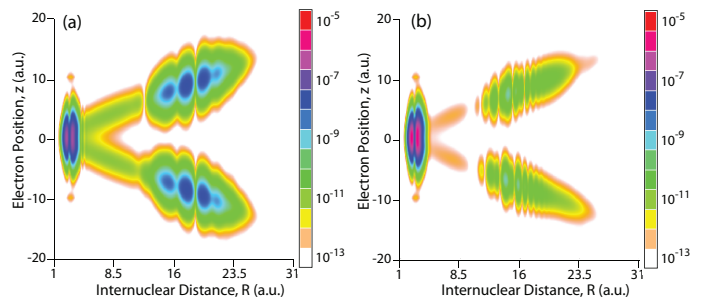


FIG. 5: (Color online) Electron probability density (after removal of the electronic-vibrational ground state) following the interaction with pump laser pulses at 800 nm with a peak intensity around  $10^{13}$  W/cm<sup>2</sup> and having a full pulse length of (a) 1 cycle (i.e. 2.7 fs) at 23.564 fs and (b) 3 cycles (i.e. 8.1 fs) at 25.872 fs.

pulses with longer pulse lengths as well as with different frequencies in order to explore the parameter regime of the pump pulse for creating a well-confined two-center scenario in the dissociating molecular ion. In Fig. 4 we present the excited state probability density generated by different pump pulses of 5 and 20 fs, which are resonant with the  $\sigma_g - \sigma_u$  transition. While the wavepacket generated with the 5 fs pulse is still well confined at large internuclear distance, we observe that the spread of the wavepacket is significantly larger after excitation with a 20 fs pulse. This is due to the fact that for longer pulses, the (effective) interaction time between the molecular ion and the pump pulse increases. Consequently, the width of the initial wavepacket created in the excitation step increases, which leads to a wider wavepacket at larger internuclear distances. Please note that both these pulses create a significant amount of vibrational excitation in the bound molecular ion (cf. density at small internuclear distances in Fig. 4).

For the sake of comparison, we show in Fig. 5 the corresponding excited state probability densities generated by the interaction with a non-resonant pump laser pulse operating at 800 nm and total pulse lengths of (a) 1 cycle (2.7 fs) and (b) 3 cycles (8.1 fs). At this wavelength it is well-known that the dissociation of  $H_2^+$  occurs via other mechanisms such as above threshold dissociation [38], bond softening [39, 40], or bond hardening [41]. Instead of one (narrow or wide) wavepacket, as in the case of a resonant one-photon excitation with the VUV pulses, we observe a train of nuclear wave packets for both pulse lengths. Also, in this case the vibrational states are much more excited than in the case of an excitation by the VUV pulses.

We may summarize our results so far in view of our goal to observe double-slit interference effects from the dissociating hydrogen molecular ion. For this goal, we require a single well-confined nuclear wavepacket, which corresponds to a narrow distribution of the internuclear distances (which shows certain similarities with a double-slit having a well-defined separation of the slits). From

the results presented above, we conclude that the system should be prepared in the vibrational ground state, the pump pulse should be in resonance with the  $\sigma_g - \sigma_u$  transition (in order to avoid trains of wavepackets as in the case of dissociation driven by the 800 nm pulses) and as short as possible (in order to confine the initial wavepacket as much as possible). Furthermore, we infer from our result for the velocity of the nuclear wavepacket (cf. Fig. 3(b)) that the ionizing probe pulse should be less than about 2 fs. Otherwise the wavepacket sweeps over a rather large region of internuclear distances during the interaction with the probe pulse which will likely smear out any interference patterns in the ionization signal, as long as the internuclear distance at the moment of ionization is not detected in the experiment.

#### IV. PHOTOIONIZATION OF DISSOCIATING $\text{H}_2^+$ MOLECULE

In this section we present the results of numerical simulations in which we took the complete pump-probe scheme into account (Fig. 1). First, we focus on the identification of interference patterns in the yields of ionization of the dissociating hydrogen molecular ion by a time-delayed probe pulse and then we analyze the results in view of an imaging of the nuclear wave packet. For our analysis we used an ultrashort dissociating pump pulse, resonant with the  $\sigma_g - \sigma_u$  transition ( $\omega_d = 0.38$  a.u.,  $\lambda = 117$  nm) and a full pulse length of 48.66 a.u. (1.2 fs, or 3-cycles) and a peak intensity of  $8.4 \times 10^{12}$  W/cm<sup>2</sup>. The corresponding dissociation dynamics of the model  $\text{H}_2^+$  is represented by the results shown in Figs. 2 and 3. In each simulation, we project out the ground state of the  $\text{H}_2^+$  model ion after the interaction with the pump pulse, assuming that any ionization signal from the bound molecular ion can be well separated in the experiment.

##### A. Double-slit interferences

We performed a series of numerical simulations in which we considered the application of a second photoionizing probe pulse as a function of time delay  $\tau$ . After the end of the probe pulse we calculated the ionization yield via the integral over the outgoing parts of the electron wave packet as (please note, that we projected out the ground state of the  $\text{H}_2^+$  model after the pump step):

$$P^+ = \lim_{t \rightarrow \infty} \int_0^\infty dR \int_{|z|=10+\frac{R}{2}}^\infty dz |\Psi(z, R, t)|^2. \quad (5)$$

We continued the propagation of the wavefunction until the ionization signal determined on the grid did not change as a function of time.

According to previous analysis the photoionization yield from a diatomic molecule is expected to be mod-

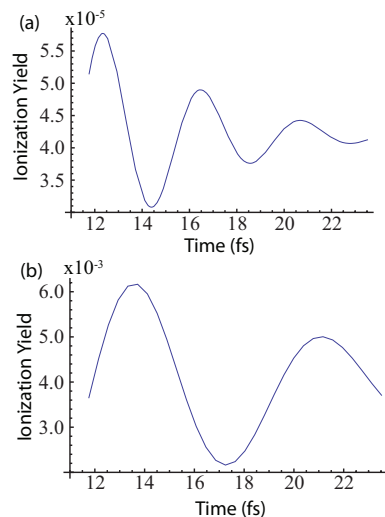


FIG. 6: (Color online) Results of numerical simulations for the ionization yield using two different wavelengths for the ionizing pulse: (a) 22 nm and (b) 45 nm.

ulated as [2, 13]:

$$P^+(\mathbf{k}, \mathbf{R}) \propto 1 + \cos(\mathbf{k} \cdot \mathbf{R} + \Phi(\mathbf{k}, \mathbf{R})), \quad (6)$$

with  $\Phi(\mathbf{k}, \mathbf{R}) = \phi_{\text{orb}} + \phi_{\text{scat}}(\mathbf{k}, \mathbf{R})$ , where  $\phi_{\text{orb}}$  accounts for the phase of the symmetry of the orbital from which the electron is emitted ( $\phi_{\text{orb}} = \pi/2$  for the present case, as the electron is in the  $\sigma_u$ -orbital), and  $\phi_{\text{scat}}(\mathbf{k}, \mathbf{R})$  represents a phase acquired due to the scattering of the electron by the neighboring proton [13]. Since the symmetry of the electronic molecular wavefunction does not change during the dissociation,  $\phi_{\text{orb}}$  does not depend on the internuclear distance and the photoelectron momentum. In contrast, one may expect that in general the acquired scattering phase depends on both these parameters. Since in our calculations we restricted the electron motion to one dimension along the internuclear axis of the molecular ion, Eq. (6) reduces to:

$$P^+(k, R) \propto 1 + \cos(kR + \Phi(k, R)). \quad (7)$$

We considered two different ionizing pulses. The first one had a frequency of  $\omega_i = 2.07$  a.u. (56.33 eV per photon), corresponding to a wavelength of 22 nm and a period of  $T_i = 3.03$  a.u. (73 as),  $N_i = 10$  (i.e., full pulse length of 730 as) and  $A_i = 0.03$  a.u. (i.e., peak intensity of  $1.35 \times 10^{14}$  W/cm<sup>2</sup>). The parameters of the second pulse were  $\omega_i = 1.01$  a.u. (27.54 eV per photon), corresponding to a wavelength of 45 nm and a period of  $T_i = 6.20$  a.u. (150 as). The number of cycles was  $N_i = 10$  (i.e., full pulse length of 1.5 fs) and the amplitude of the vector potential was  $A_i = 0.06$  a.u. (i.e., peak intensity of  $1.3 \times 10^{14}$  W/cm<sup>2</sup>).

In Fig. 6 we show the numerical results for the ionization yield as a function of the pump-probe time delay for the two ionizing pulses. We clearly observe oscillations of the ionization yields due to the interferences

of the partial electron wave packets. The amplitudes of the oscillations decrease, which we attribute to the spreading of the nuclear wavepacket (for further analysis, see section IV.B.). Over the range of time delays studied, the frequency of the oscillations remains practically constant ( $0.020 \pm 0.001$  a.u. for ionization at 45 nm, and  $0.038 \pm 0.005$  a.u. at 22 nm). Since the ionization potential of the dissociating hydrogen molecule in the present range of internuclear distance does vary very little and, hence, the photoelectron momentum remains almost constant, we conclude that the phase  $\Phi$  and, hence, the scattering phase  $\phi_{\text{scat}}$  is independent of the internuclear distance  $R$  (or, of the time delay  $\tau$ ). This result makes sense, since in the present model we restricted the electron motion to one dimension along the internuclear distance and at large internuclear distances the Coulomb potentials located at the two protons are well separated and vary just slightly with an increase of  $R$ . Thus, the scattering process of the electron at the neighboring Coulomb potential is (almost) independent of the value of  $R$  and, hence,  $\Phi(k, R) = \Phi(k)$  for large  $R$  in our model.

Before we proceed, we may mention that we have also considered probing the dissociating molecular ion using near-infrared laser pulses at 800 nm. Due to the non-perturbative coupling between the electron and field at this wavelength, the ionization of the electron proceeds via tunneling or multiphoton above-threshold ionization. Consequently, the electron is not emitted at a given energy (within a certain width) but with a range of electron energies that is rather broad. In order to observe any trace of the double-slit interference as a function of the internuclear distance, it is therefore necessary to restrict the electron energy in an experiment as well as in the numerical simulations. In other words, instead of total ionization yields, we have to obtain partial differential ionization yields

$$\Delta P^+ = (dP^+/dk)\Delta k. \quad (8)$$

Furthermore, the period of a near-infrared field is about 2.7 fs, over which the expectation value of the nuclear wavepacket changes by more than 2 a.u. (see, Fig. 3). As long as the internuclear distance is not (indirectly) observed in an experiment, any interference effects will therefore smear out for near-infrared probe pulses with a few cycles of duration. Finally, strong-field ionization effects, such as rescattering [42] and multiple ionization bursts per half cycle of the field [43], are other obstacles for the occurrence of the double-slit interference effects in the partial differential ionization yields.

Assuming an ideal scenario, in which the dissociating hydrogen molecular ion is ionized by an 800 nm laser pulse with just one cycle (total pulse length of 2.7 fs), we have performed numerical simulations for a pulse with a peak of the vector potential of  $A_{0,i} = 3$  a.u. (about  $10^{15}$  W/cm<sup>2</sup> peak intensity). As shown in Fig. 7, we observe a characteristic oscillation in the partial differential ionization yield at a specific value of the photoelectron

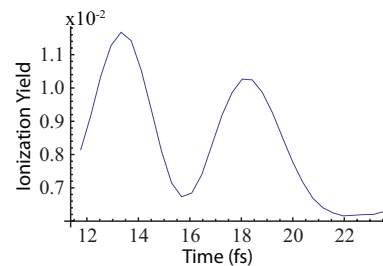


FIG. 7: (Color online) Results of numerical simulations for the partial differential ionization yield of  $\text{H}_2^+$  interaction with a 1-cycle pulse at 800 nm. The photoelectron linear momentum was selected as  $k_0 = -1.36$  a.u. and a detector resolution of  $\Delta k = 0.1$  a.u. was considered.

momentum of  $k_0 = -1.36$  a.u.. The negative sign indicates that the electron is emitted in direction opposite to the laser polarization direction. We note that the yield for electrons emitted with the same absolute momentum value in the laser polarization direction, as well as the yields at different electron momenta, do not show any characteristic oscillatory behaviour. Thus, despite the fact that the oscillation in the specific yield in Fig. 7 appears to resemble the interference patterns, we expect that in general interference effects cannot be observed using a intense probe laser pulse at near-infrared wavelengths.

## B. Imaging of nuclear wavepacket dynamics

Now, we will analyze which information about the dissociating nuclear wave packet (velocity, spreading, etc.) can be retrieved from the double-slit interference patterns. For large internuclear distances we can well approximate

$$kR(\tau) + \Phi \approx 2k v \tau + kR_c + \Phi \quad (9)$$

where  $v$  is the velocity of the dissociating protons and  $kR_c$  is a phase that depends on the initial internuclear distance and the initial acceleration due to the repulsive potential at small internuclear distances. Thus, the frequencies of the oscillations in Fig. 6 are approximately equal to  $2kv$  and we can retrieve the velocity (or momentum) of the protons. From the results of our simulations for the 45 nm ionizing pulse, we read a frequency of 0.020 a.u. ( $\pm 0.001$  a.u.), while the photoelectron momentum is  $k = 0.83$  a.u. ( $\pm 0.02$  a.u.), obtained from the Fourier transform of the ionized photoelectron wave functions in the simulations. This gives rise to a velocity of  $v = 0.012$  a.u. ( $\pm 0.001$  a.u.). For the 22 nm ionizing pulse we obtain a frequency of 0.038 a.u. ( $\pm 0.005$  a.u.) and a momentum of  $k = 1.64$  a.u. ( $\pm 0.02$  a.u.), resulting in a velocity of  $v = 0.011$  a.u. ( $\pm 0.001$  a.u.). Both results are in good agreement with the velocity of  $v = 0.0104$  a.u. ( $\pm 0.0003$  a.u.) obtained from the results for the expecta-

tion value of the internuclear distance  $\langle R \rangle$ , shown in Fig. 2(b).

As outlined before, the decay of the oscillations in Fig. 6 depends on both the spread of the nuclear wavepacket in the internuclear distance, which increases with  $\tau$ , and the width of photoelectron momentum distributions, which remains constant with  $\tau$  in the present study. To estimate the decay we revise the formula for the double-slit interferences, given in Eq. (7), to account for the spreading as:

$$P^+(k_0, R_0) \propto \int_{-\infty}^{\infty} \int_{-\infty}^{\infty} dk dR \quad (10)$$

$$[1 + \cos(kR + \Phi)] G(R - R_0, \Delta R) G(k - k_0, \Delta k)$$

where  $G(a, b)$  is a Gaussian profile defined as

$$G(a, b) = \frac{1}{\sqrt{2\pi} b} e^{-\frac{a^2}{2b^2}}, \quad (11)$$

with  $R_0 \equiv \langle R \rangle$  being the mean value of the internuclear distance (see Fig. 2(b) for its dependence on  $\tau$ ),  $\Delta R$  is the width of the nuclear wavepacket (which depends on  $\tau$  as well),  $k_0$  and  $\Delta k$  are the center and the width of the photoelectron momentum distribution, respectively (in an actual experiment,  $\Delta k$  may also be related to the resolution of the detector). Assuming that  $\Phi$  does not depend on the internuclear distance and the central photoelectron momentum is constant, we perform the integrations in Eq. (10) to get:

$$P^+(k_0, R_0) \propto \left[ 1 \pm \frac{1}{\Delta} \cos \left( \frac{k_0 R_0}{\Delta^2} + \Phi \right) e^{-\frac{R_0^2 \Delta k^2 + k_0^2 \Delta R^2}{2\Delta^2}} \right], \quad (12)$$

where  $\Delta = \sqrt{1 + \Delta k^2 \Delta R^2}$ .  $k_0$  and  $\Delta k$  are parameters, which can be retrieved in an actual experiment (here, we take these parameters from the results of our numerical simulations). Thus, we are left with two variables in Eq. (12), namely the internuclear distance  $R_0$  and the spreading of the nuclear wavepacket  $\Delta R$ . As explained before, at large internuclear distances the Coulomb repulsion between the two protons becomes negligible and the protons propagate with constant momentum. In this regime we get

$$R_0(\tau) \approx 2v\tau + R_c \quad (13)$$

and

$$\Delta R(\tau) \approx \sqrt{1 + 4\tau^2 \Delta k_p^4 / m_p^2} / (2\Delta k_p) + \Delta R_c, \quad (14)$$

where  $\Delta k_p$  is the spreading of the relative momentum of the protons and  $m_p = 918$  a.u. is the reduced mass of the two protons.  $\Delta R_c$  and  $R_c$  are two terms which account for the initial nuclear spread, the initial internuclear distance and the initial acceleration of the protons, where the linear temporal approximation fails due to the strong repulsive Coulomb potential. As shown before,  $v$  can be

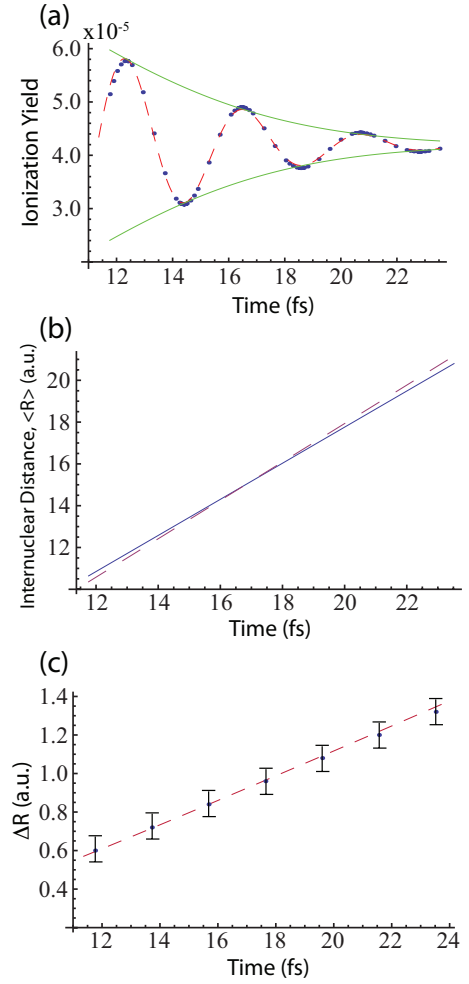


FIG. 8: (Color online) (a) Ionization yields: Comparison between the results of numerical simulations (blue points) and the predictions of the analytical model, Eq. (12), with (red dashed line) and without (green solid line) the cos-term, choosing  $v = 0.0111$  a.u.,  $k = 1.64$  a.u.,  $\Delta k = 0.084$  a.u.,  $\Delta k_p = 1.48$  a.u.,  $R_c = -0.45$  a.u.,  $\Delta R_c = -0.26$  a.u. and  $\Phi = 1$  a.u.. (b) Mean value of the internuclear distance: Comparison between the results of numerical simulations (blue solid line) and the fit formula, Eq. (13) (red dashed line). (c) Spreading of the nuclear wavepacket: Comparison between the results of numerical simulations (points with error bars due to the grid resolution) and the fit formula, Eq. (14) (red dashed line).

retrieved with high accuracy from the interference pattern. Assuming that  $\Delta k_p$  can be either observed in the experiment or approximately retrieved from the width of the photoelectron momentum distribution, we need to fit the two parameters  $R_c$  and  $\Delta R_c$  to obtain (the mean value of) the internuclear distance and the width of the nuclear wave packet at the moment of ionization from the decay of the oscillations.

In order to check our analytical model, we performed numerical simulations for the 22 nm ionizing pulse with a high resolution of the time delay ( $\Delta\tau = 0.04$ ,  $T_d = 15$

as) (cf. points in Fig. 8(a)). Choosing  $R_c = -0.45$  a.u. and  $\Delta R_c = -0.26$  a.u. we obtain a very good fit of the decay of the amplitudes of the oscillations (see green solid curves in Fig. 8(a)). Using these parameters and choosing  $\Phi=1$  rad, we were also able to fit the detailed oscillations very well (red dashed curve). As explained above, the fitting procedure allows us to further retrieve the mean value of the internuclear distance and the width of the nuclear wave packets. In Figs. 8(b) and (c), we compare the results of these fits (red dashed lines) with the results retrieved from our numerical simulations (blue solid lines and points). The agreement is very satisfactory. Therefore, we can expect to be able to extract dynamical information about the nuclear wavepacket from such interference patterns in an experiment.

## V. SUMMARY

We have studied double-slit like interferences in the photoionization yields of a dissociating hydrogen molecular ion via numerical simulations of the time-dependent Schrödinger equation. To this end, we analyzed the different steps in a pump-probe scenario, in which  $\text{H}_2^+$  is excited by a pump pulse from the ground state to the first excited dissociative state and is then probed by a second time-delayed pulse, which ionizes the electron from the molecular ion as the ion dissociates. The results of our numerical simulations for a  $\text{H}_2^+$  model ion in its vibra-

tional ground state show that the frequency of the pump pulse should be in resonance with the  $\sigma_g - \sigma_u$  transition and should not be longer than about 5 fs in duration (total pulse duration) in order to generate a well confined nuclear wavepacket, which is a requirement to observe interference effects in the dissociating molecular ion (as long as the internuclear distance of the protons at the moment of ionization is not observed). We have shown that the yields of ionization due to the interaction with a VUV probe pulse exhibit the expected double-slit interferences as a function of time delay between the two pulses. The amplitudes of the oscillation are found to decrease with increase of the time delay due to the spreading of the wave packet. By developing an analytical model we were able to retrieve information about the nuclear wavepacket, namely its velocity, the mean value of the internuclear distance and the width of the wavepacket, from the oscillations in the ionization yields. We have tested the predictions of the analytical model against the results of numerical simulations and found a very satisfactory agreement.

## Acknowledgements

AP acknowledges financial support from the Spanish Ministry of Science and Innovation through their Post-doctoral program. The work was partially supported by NSF.

- 
- [1] T. Young, Proc. Roy. Soc. Long. A **94**, 1 (1804).
  - [2] H.D. Cohen and U. Fano, Phys. Rev. **150**, 30 (1966).
  - [3] J.A.R. Samson and R.B. Cairns, J. Opt. Soc. Am. **55**, 1035 (1965).
  - [4] O.A. Fojón, J. Fernandez, A. Palacios, R.D. Rivaola, and F. Martin, J. Phys. B **37**, 3035 (2004).
  - [5] G.L. Yudin, S. Chelkowski, and A.D. Bandrauk, J. Phys. B **39**, L17 (2006).
  - [6] J. Fernandez, O. Fojón, A. Palacios, and F. Martin, Phys. Rev. Lett. **98**, 043005 (2007).
  - [7] J. Fernandez, O. Fojón, and F. Martin, Phys. Rev. A **79**, 023420 (2009).
  - [8] R. Della Picca, P.D. Fainstein, M.L. Martiarena, N. Sisourat, and A. Dubois, Phys. Rev. A **79**, 032702 (2009).
  - [9] J. Fernandez, F.L. Yip, T.N. Rescigno, C.W. McCurdy, and F. Martin, Phys. Rev. A **79**, 043409 (2009).
  - [10] S.X. Hu, L.A. Collins, and B.I. Schneider, Phys. Rev. A **80**, 023426 (2009).
  - [11] D. Rolles, M. Braune, S. Cvejanovic, O. Geßner, R. Hentges, S. Korica, B. Langer, T. Lischke, G. Prümper, A. Reinköster, J. Viehhaus, B. Zimmermann, V. McKoy, and U. Becker, Nature **437**, 711 (2005).
  - [12] S.K. Semenov, N.A. Cherepkov, M. Matsumoto, T. Hata-moto, X.-J. Liu, G. Prümper, T. Tanaka, M. Hoashino, H. Tanaka, F. Gel'mukhanov, and K. Ueda, J. Phys. B **39**, L261 (2006).
  - [13] X.-J. Liu, N.A. Cherepkov, S.K. Semenov, V. Kimberg, F. Gel'mukhanov, T. Lischke, T. Tanaka, M. Hoshino, H. Tanaka, and K. Ueda, J. Phys. B **39**, 4801 (2006).
  - [14] N.A. Cherepkov, S.K. Semenov, M.S. Schöffler, J. Titze, N. Petridis, T. Jahnke, K. Cole, L.Ph.H. Schmidt, A. Czasch, D. Akoury, O. Jagutzki, J.B. Williams, T. Osipov, S. Lee, M.H. Prior, A. Belkacem, A.L. Landers, H. Schmidt-Böcking, R. Dörner, and Th. Weber, Phys. Rev. A **82**, 023420 (2010).
  - [15] N. Stolterfoht, B. Sulik, V. Hoffmann, B. Skogvall, J.Y. Chesnel, J. Rangama, F. Frémont, D. Hennecart, A. Cassimi, X. Husson, A.L. Landers, J.A. Tanis, M.E. Galassi, and R.D. Rivaola, Phys. Rev. Lett. **87**, 023201 (2001).
  - [16] D. Misra, U. Kadhane, Y.P. Singh, L.C. Tribedi, P.D. Fainstein, and P. Richard, Phys. Rev. Lett. **92**, 153201 (2004).
  - [17] C.R. Stia, O.A. Fojón, P.F. Weck, J. Hanssen, and R.D. Rivaola, J. Phys. B **36**, L257 (2003).
  - [18] O. Kamalou, J.-Y. Chesnel, D. Martina, J. Hanssen, C.R. Stia, O.A. Fojón, R.D. Rivaola, F. Frémont, Phys. Rev. A **71**, 010702(R) (2005).
  - [19] M. Walter and J. Briggs, J. Phys. B **32**, 2487 (1999).
  - [20] D. Akoury, K. Kreidi, T. Jahnke, Th. Weber, A. Staudte, M. Schöffler, N. Neumann, J. Titze, L.Ph.H. Schmidt, A. Czasch, O. Jagutzki, R.A. Costa Fraga, R.E. Grisenti, R. Diez Muino, N.A. Cherepkov, S.K. Semenov, P. Ranitovic, C.L. Cocke, T. Osipov, H. Adaniya, J.C. Thompson, M.H. Prior, A. Belkacem, A.L. Landers, H. Schmidt-



- Böcking, and R. Dörner, *Science* **318**, 949 (2007).
- [21] K. Kreidi, D. Akoury, T. Jahnke, Th. Weber, A. Staudte, M. Schöffler, N. Neumann, J. Titze, L.Ph.H. Schmidt, A. Czasch, O. Jagutzki, R.A. Costa Fraga, R.E. Grisenti, M. Smolarski, P. Ranitovic, C.L. Cocke, T. Osipov, H. Adaniya, J.C. Thompson, M.H. Prior, A. Belkacem, A.L. Landers, H. Schmidt-Böcking, and R. Dörner, *Phys. Rev. Lett.* **100**, 133005 (2008).
- [22] D.A. Horner, S. Miyabe, T.N. Rescigno, C.W. McCurdy, F. Morales, and F. Martin, *Phys. Rev. Lett.* **101**, 183002 (2008).
- [23] M. Schöffler, K. Kreidi, D. Akoury, T. Jahnke, A. Staudte, N. Neumann, J. Titze, L.Ph.H. Schmidt, A. Czasch, O. Jagutzki, R.A. Costa Fraga, R.E. Grisenti, M. Smolarski, P. Ranitovic, C.L. Cocke, T. Osipov, H. Adaniya, S. Lee, J.C. Thompson, M.H. Prior, A. Belkacem, Th. Weber, A. Landers, H. Schmidt-Böcking, and R. Dörner, *Phys. Rev. A* **78**, 013414 (2008).
- [24] A. Rüdél, R. Hentges, U. Becker, H.S. Chakraborty, M.E. Madjet, and J.M. Rost, *Phys. Rev. Lett.* **89**, 125503 (2002).
- [25] J. Muth-Böhm, A. Becker, and F.H.M. Faisal, *Phys. Rev. Lett.* **85**, 2280 (2000).
- [26] A. Jarón-Becker, A. Becker, and F.H.M. Faisal, *Phys. Rev. Lett.* **96**, 143006 (2006).
- [27] A.V. Davis, R. Wester, A.E. Bragg, and D.M. Neumark, *J. Chem. Phys.* **118**, 999 (2003).
- [28] R. Mabbs, K. Pichugin, and A. Sanov, *J. Chem. Phys.* **122**, 174305 (2005).
- [29] R. Mabbs, K. Pichugin, and A. Sanov, *J. Chem. Phys.* **123**, 054329 (2005).
- [30] S. Chelkowski and A.D. Bandrauk, *Phys. Rev. A* **81**, 062101 (2010).
- [31] J.R. Hiskes, *Phys. Rev.* **122**, 1207 (1961).
- [32] K.C. Kulander, F.H. Mies, and K.J. Schafer, *Phys. Rev. A* **53**, 2562 (1996).
- [33] J. Crank and P. Nicolson, *Proc. Camb. Phil. Soc.* **43**, 50 (1947).
- [34] S. Chelkowski, T. Zuo, O. Atabek, and A.D. Bandrauk, *Phys. Rev. A* **52**, 2977 (1995).
- [35] V. Roudnev, B.D. Esry, and I. Ben-Itzhak, *Phys. Rev. Lett.* **93** 163601 (2004).
- [36] F. He, C. Ruiz, and A. Becker, *Phys. Rev. Lett.* **99**, 083002 (2007).
- [37] F. He, A. Becker, and U. Thumm, *Phys. Rev. Lett.* **101**, 213002 (2008).
- [38] A. Giusti-Suzor, X. He, O. Atabek, and F.H. Mies, *Phys. Rev. Lett.* **64**, 515 (1990).
- [39] A.D. Bandrauk and M.L. Sink, *J. Chem. Phys.* **74**, 1110 (1981).
- [40] P.H. Bucksbaum, A. Zavriyev, H.G. Muller, and D.W. Schumacher, *Phys. Rev. Lett.* **64**, 1883 (1990).
- [41] L.J. Frasinski, J.H. Posthumus, J. Plumridge, K. Codling, P.F. Taday, and A.J. Langley, *Phys. Rev. Lett.* **83**, 3625 (1999).
- [42] P.B. Corkum, *Phys. Rev. Lett.* **71**, 1994 (1993).
- [43] N. Takemoto and A. Becker, *Phys. Rev. Lett.* in press (arXiv:1009.2868v1).